RSC Advances

ROYAL SOCIETY OF CHEMISTRY

www.rsc.org/advances

Fabrication of mechanically durable superhydrophobic wood surfaces using polydimethylsiloxane and silica nanoparticles

Huanjun Chang, Kunkun Tu, Xiaoqing Wang* and Junliang Liu

Research Institute of Wood Industry, Chinese Academy of Forestry, Beijing 100091, P. R. China.

E-mail: wangxq@caf.ac.cn.

Abstract: The excellent properties of wood utilized as an engineering material are detracted by the complex wood-water interactions and the resulting dimensional instability and low durability against biological degradation. Inspired by the lotus effect, mechanically durable superhydrophobic coatings were successfully fabricated on the intrinsically heterogeneous wood substrates by simply dip-coating the suspensions of hydrophobic silica (SiO_2) nanoparticles dispersed in polydimethylsiloxane (PDMS) solution. A subsequent low-surface-energy treatment with some expensive reagents is not necessary owing to the hydrophobic nature of PDMS and the modified silica particles. The surface microstructure, roughness and wetting behavior of the PDMS/silica hybrid coatings on wood surfaces were investigated in relation to the loadings of the silica particles in the PDMS matrix. When the silica particle loading reached a critical level, desirable hierarchical micro/nanostructures were formed on the wood substrate, allowing for the generation of superhydrophobicity with a contact angle of 152° and a sliding angle less than 10°. The fabricated PDMS/silica hybrid coating exhibited desirable durability against mechanical abrasion and high-frequency ultrasonic washing in water whilst basically retaining its microstructure and superhydrophobicity. Such mechanically durable superhydrophobic wood surfaces with self-cleaning properties offer an interesting alternative for wood modification, and could improve the performance of wood as an engineering material.

Keywords: wood, superhydrophobicity, PDMS, silica nanoparticle, hybrid coating, mechanical abrasion

Introduction

Wood has long been used as an important engineering material owing to its excellent mechanical properties, aesthetic appeal, and environmental friendliness. However, due to the hydroscopic nature of amorphous cellulose and hemicelluloses in the cell walls, wood shrinks or swells upon changes in moisture contents which can lead to substantial deformations (*e.g.* distortion, twisting and cracking) of construction elements. The presence of high moisture also encourages colonial growth of fungi in wood, resulting in degradation of cell walls and low durability of wood in service.

Accordingly, many attempts have been made to improve the hydrophobicity of wood. The transformation of wood from hydrophilicity to hydrophobicity mainly involves using reactive chemicals to block hydroxyl groups of cell wall polymers to reduce water sorption sites in wood, or incorporation of materials into the cell wall to fill microvoids within it, thereby occupying space that would otherwise be available to water molecules, such as acetylation,[1,2] silanization,[3,4] *in-situ* polymerization, [5,6] and flavonoid insertion into cell walls.[7] Although these methods can be used to reduce or delay water/moisture absorption into wood, they cannot prevent water absorption upon direct exposure of wood to liquid water. Moreover, such bulk hydrophobization of wood in deeper layers is usually complex, costly and undesirable due to the complicated structure of wood. Hence, surface modification and functionalization could be an interesting alternative.

Nature has offered many examples of superhydrophobic surfaces exhibiting great water-repellent properties with water contact angles higher than 150°, such as plant leaves,[8] rose petals,[9] and water strider's legs.[10] Superhydrophobic surfaces have been attracting considerable attention since they possess not only excellent water-repellency but also show self-cleaning, anti-icing and anti-corrosive properties, and have great potential in various applications.[11-15] Superhydrophobic surfaces are expected to minimize wood-water interactions and thus avoid problems associated with water absorption. Such system may serve as a desirable solution for wood protection against water. It has been suggested that the superhydrophobic properties are a result of suitable hierarchical micro- and nano-structures of the surface superimposed with materials with low surface free energy.[16]

Wood substrate is intrinsically heterogeneous due to its surface anatomical structure and

porosity, forming primary roughness at the microscale. With the microscale roughness inherent on the wood substrate, it is feasible to develop dual-scale roughness to fabricate superhydrophobic wood surfaces by incorporating nanoscale materials coupled with low-surface-energy treatments. Recently, artificial superhydrophobic coatings have been successfully developed on solid woods by using various techniques to control the surface structure and roughness, such as sol-gel process,[17,18] hydrothermal method,[19,20] wet chemical method,[21,22] and plasma treatment.[23] However, even with attractive nonwetting properties, the fabricated superhydrophobic wood surfaces are not suitable for practical uses in real-life conditions because of the limited mechanical stability and durability of the coatings. Without proper design, the surface hydrophobic layers and the underlying topographical patterns of the superhydrophobic surfaces are prone to be damaged by mechanical abrasion, leading to undesired pinning of water droplets on the surface and loss of water-repellency. The practical application of superhydrophobic surfaces relies on wetting robustness of the products as well as simple and inexpensive fabrication processes.

In this study, we present a simple and inexpensive dip-coating method to fabricate mechanically durable superhydrophobic coating on the heterogeneous wood surfaces using polydimethylsiloxane (PDMS) and silica nanoparticles, both of which are inexpensive and environmentally friendly. As illustrated in Fig. 1, hydrophobic silica particles were prepared by hydrolysis and condensation of tetraethoxysilane (TEOS) under an alkaline condition, followed by hydrophobic modification with hexadecyltrimethoxysilane (HDTMS) to graft long-chain alkyl group onto the surface. The HDTMS-coated silica particles were then dispersed into PDMS solutions to form PDMS-silica suspensions, which were subsequently applied onto wood surfaces by dip-coating (other techniques like spray-coating can also be used for large-area fabrication). Heat treatment transformed the applied solutions into organic-inorganic hybrid coatings having hierarchical nanotextured surface morphology, which was readily controlled by adjusting the mass ratio of silica to PDMS. The as-prepared superhydrophobic wood surfaces showed desirable mechanical stability and durability against abrasion damage and high-frequency ultrasonic washing in water.

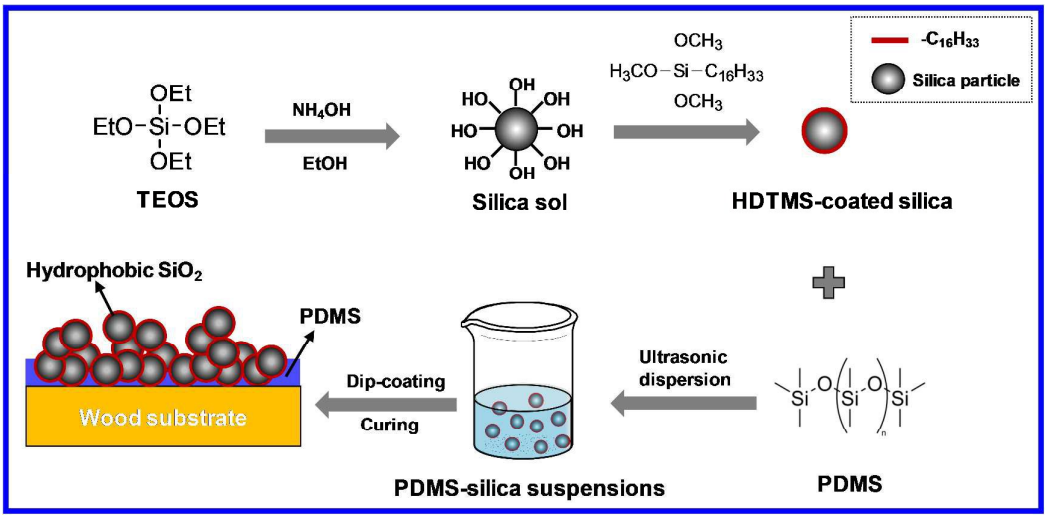

Fig. 1 Schematic illustration of the procedure to fabricate PDMS-silica hybrid superhydrophobic coatings on the wood substrate.

Experimental

Materials

Tetraethoxysilane (TEOS) and hexadecyltrimethoxysilane (HDTMS) were obtained from Sigma-Aldrich (St. Louis, Minnesota, USA). Ammonium hydroxide (NH_4OH, 25%), tetrahydrofuran (THF) and ethanol were purchased from Sinopharm Chemical Reagent Co., Ltd (Shanghai, China). Polydimethylsiloxane (PDMS Sylgard 184) and the corresponding curing agent were supplied by Dow Corning (Michigan, USA). All chemicals were used as received without further purification. Wood samples of Chinese fir (*Cunninghamia lanceolata*) were cut parallel to grain direction and sawn into blocks of 20 mm × 20 mm × 5 mm (radial × longitudinal × tangential).

Synthesis of hydrophobic silica particles

Monodisperse silica sols were firstly synthesized by a typical Stöber method. Briefly, NH_4OH (3 ml) and ethanol (50 ml) were mixed to form a homogeneous solution with magnetic stirring for 30 min at 50 °C, and TEOS (3 ml) was then added dropwise into the above solution while stirring, which was continued for 2 h to form a transparent silica sol. After that, 1% HDTMS was added into the sol system in order to modify the hydrophilic silica particles. The reaction was allowed to continue for another 2 h under magnetic stirring at 50 °C to form a hydrophobic silica sol. The

silica particles were then collected by centrifugation (10,000 rpm, 12 min), and re-dispersed in ethanol. After three centrifugation and re-dispersion cycles, the particles were finally vacuum-dried for 10 h.

Preparation of coating solutions

PDMS/THF solution was firstly prepared as follows: PDMS (0.55g) was mixed with THF (30 ml) with magnetic stirring for 30 min at room temperature to form the solution A, and the corresponding curing agent (0.055 g) was dissolved to THF (30 ml) to form the solution B. The solutions A and B were mixed together to form a PDMS/THF solution (1%, w/w). Different amounts of the HDTMS-modified silica particles (with SiO_2/PDMS mass ratio of 1:1, 2:1, 3:1 and 4:1, respectively) were then dispersed in the as-prepared PDMS/THF solution with the aid of ultrasonication for 1 h to form coating solutions.

Preparation of superhydrophobic coatings on wood substrates

Prior to the coating treatment, the wood samples were ultrasonically washed with ethanol for 10 min and dried at 60 °C for 6 h. The cleaned samples were then dipped into the as-prepared coating solutions for ~10 min, and dried at 103 °C for 1 h. This procedure was repeated for 3 times to allow full deposition of PDMS/SiO_2 composites on wood surfaces and to achieve adequate thickness of the hybrid coatings. The coated wood samples were finally ultrasonically washed in ethanol to remove the free or loosely attached nanoparticles, and dried at 103 °C for 5 h.

Microstructure and morphology of the hybrid coatings

The HDTMS-modified silica particles were observed by transmission electron microscopy (TEM, Tecnai G2 F30, FEI, USA). Fourier transform infrared spectroscopy (FTIR, Nicolet Magna-IR 750, USA) was used to study qualitatively the methyl (-CH_3) and methylene (-CH_2) groups grafted on the modified silica particles. The surface structure and morphology of the hybrid coatings on wood substrates were examined using field-emission scanning electron microscopy (FE-SEM, Zeiss SUPRA 55, Germany). A thin Aurum (Au) layer was sputtered onto the sample surfaces to improve conductivity prior to observation. The surface roughness of the coatings was analyzed by atomic force microscopy (AFM, Dimension Icon, Bruker, Germany) with tapping mode. The scanning scale is 3μm ×3μm.

Hydrophobicity measurement

The hydrophobicity of the coated wood samples was evaluated by water static contact angle (CA)

and dynamic sliding angle (SA), which were measured by a contact angle meter (Shanghai Zhongchen JC2000D, China) at ambient temperature. The static CA was recorded 60 s after a water droplet (5 μl) was placed on the sample surface. The SA was determined by the minimum tilt angle at which a water droplet (15 μl) rolls off the surface. The average CA and SA values were obtained by measuring more than five positions for each sample.

Mechanical durability of the superhydrophobic coatings

In order to examine the abrasion resistance of the superhydrophobic wood coatings, scratch tests were performed according to the reported method.[24] As schematically illustrated in Fig. 2, With a pressure of 12.5 kPa applied, the superhydrophobic surface was scratched against sandpaper (1500 mesh) with the abrasion length of 30 cm and a speed of 3 cm/s. The scratch tests were conducted for 10 cycles, and CA and SA were measured after each abrasion cycle. Changes in surface morphology and structure of the superhydrophobic coatings during the abrasion procedure were examined by FE-SEM.

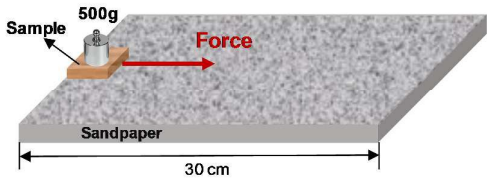

Fig. 2 Sketch of the setup used to determine the mechanical stability of the superhydrophobic surface against abrasion.

The washing durability of the superhydrophobic coatings was examined by submerging the coated wood samples in a volume of distilled water ten times that of the samples for 10 h under ultrasonication with an ultrasonic frequency of 80 kHz and ultrasonic power of 100 W. The samples were collected at certain intervals and dried at 103 °C for 5 h, followed by CA and SA measurements.

Results and discussion

Microstructure and surface morphology

The TEM images of the synthesized silica nanoparticles are shown in Fig. 3. Well-dispersed

spherical silica particles of 60~120 nm in diameter were synthesized by the Stöber method. When modified with HDTMS (1%), the silica particles were found to be coved by a thin layer of polymer-like materials (see arrows in Fig. 3b). The neighboring particles were also observed to be connected by the polymer bridge showing an obvious tendency to aggregate with each other.

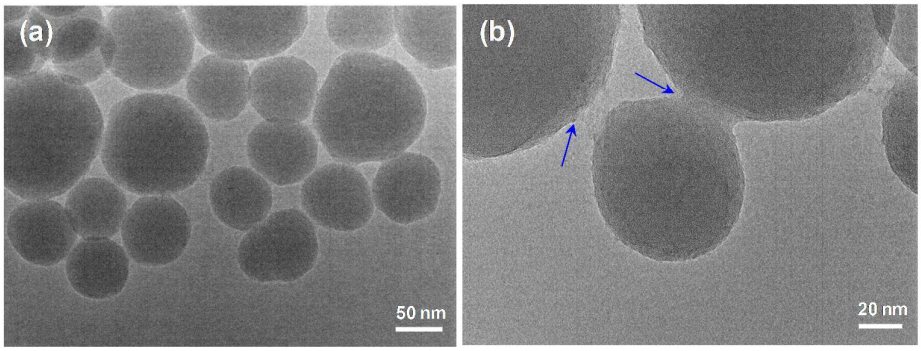

Fig. 3 TEM images of the (a) synthesized and (b) HDTMS-coated silica nanoparticles.

FT-IR was used to gain insights into the chemical structure of the formed polymer covering silica particles (Fig. 4). In the FT-IR spectra of bare silica particles, two absorption peaks were observed at 1055 and 795 cm^{-1}, which are attributed to the stretching vibration of Si-O-Si. The absorption peak at 951 cm^{-1} is ascribed to the stretching vibration of Si-OH. After HDTMS coating, two additional peaks at 2925 and 2854 cm^{-1} appeared, which are assigned to the asymmetric and symmetric stretching of the CH_2 group, respectively.[25] This indicates that the long-chain alkyl groups ($-C_{16}H_{33}$) of HDTMS were successfully grafted on the silica particle surface, confirming the results of TEM observations.

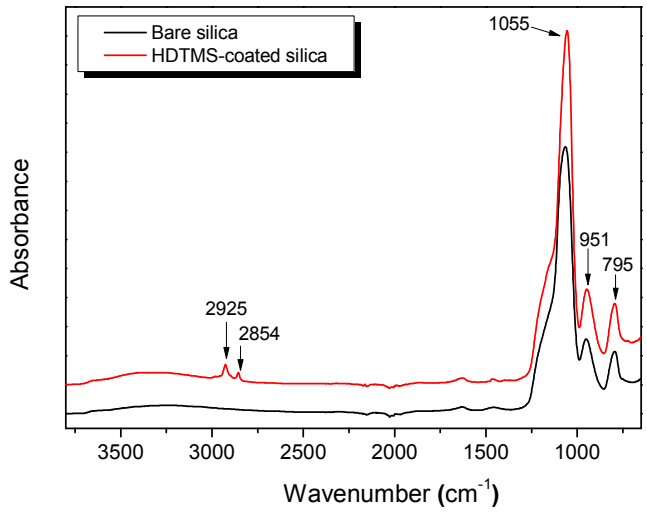

Fig. 4 FTIR spectra of bare and HDTMS-coated silica nanoparticles.

The SEM images of the wood surfaces coated with PDMS-silica nanocomposites with various mass ratios of silica to PDMS are shown in Fig. 5. When coated with PDMS only, the wood lumen surface was observed to be covered by a relatively smooth and continuous film at high magnification (Fig. 5a). The wood surface presents a highly-textured cellular structure, forming the primary roughness at the micro-scale. When a small amount of silica particles was incorporated into the coating with a silica/PDMS mass ratio of 1:1, the morphology and roughness of the lumen surface were only slightly changed since most of the silica particles appeared to be embedded in the dense PDMS film (Fig. 5b). In this case, PDMS dictates the structure and appearance of the hybrid coatings. With an increase of silica/PDMS mass ratio to 2:1, a relatively homogeneous layer of PDMS/silica hybrid coating was observed to be coated on the lumen surface, resulting in a highly roughened wood surface (Fig. 5c). The high-magnification image shows that the hybrid coating presents a well-developed hierarchical structure consisting of interconnected microdomains (aggregates of silica particles) and nanopores, in which PDMS acts as a binding agent for connecting and anchoring the silica particles. A further increase of silica/PDMS mass ratio to 3:1 resulted in a similar hybrid coating with a well-developed microstructure and a highly roughened lumen surface (Fig. 5d).

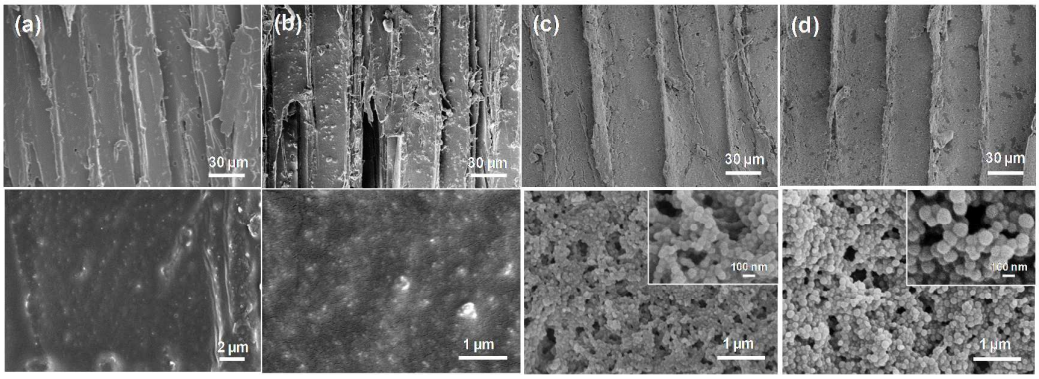

Fig. 5 SEM images of wood surfaces coated with (a) PDMS only and PDMS-silica nanocomposites with SiO_2/PDMS mass ratio of (b) 1:1, (c) 2:1 and (d) 3:1. High-magnification images display details of the coatings.

The surface morphology and roughness of the coated wood were further examined by atomic force microscopy (AFM). The three-dimensional AFM images of the wood lumen surfaces coated with PDMS-silica nanocomposites are shown in Fig. 6. The PDMS-coated wood surface was

rather smooth with R_{rms} (root-mean-square roughness) of 11.8 nm. With a small amount of silica particles incorporated, the hybrid coating surface was slightly roughened with R_{rms} of 23.5 nm (Fig. 6b). By contrast, at a relatively high silica particle loading, the well-developed hierarchical structure with microdomains and nanopores can also be observed in the AFM image with relatively high R_{rms} of 58.1 (Fig. 6c).

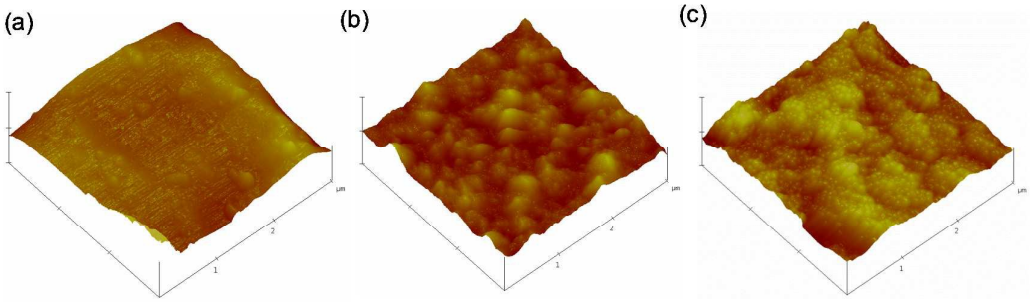

Fig. 6 Three-dimensional AFM images of the wood lumen surfaces coated with (a) PDMS only and PDMS-silica nanocomposites with SiO_2/PDMS mass ratio of (b) 1:1 and (c) 2:1.

Hydrophobicity

The water CAs and SAs were investigated to examine the hydrophobicity of the PDMS/silica hybrid coatings on wood surfaces. As shown in Fig. 7, the PDMS-coated wood already exhibited high water-repellency with a CA of ~140°, which is of course mainly attributed to the hydrophobic nature of PDMS. However, it has been shown that the maximum CA that can be achieved on a smooth surface is about 120° even when a material with the lowest surface free energy is used.[26] This indicates that the inherent microscale roughness of wood substrate also contributes to the high hydrophobicity, but applying the hydrophobic PDMS alone is not sufficient to generate superhydrophobicity on wood surfaces. When silica particles were incorporated into the PDMS film, the water-repellent properties of the coated wood were remarkably improved. With increasing silica/PDMS mass fraction from 0 to 4, the CA increased initially from 140° to 152°, then dropped slightly and remained almost constant around 150°. At low silica particle loadings, the water droplets were also found to adhere strongly to the wood surfaces with high SAs. With increasing silica particle to PDMS ratio, the SAs of the coated wood decreased considerably down to around 10° and the water droplets can roll off the surfaces easily.

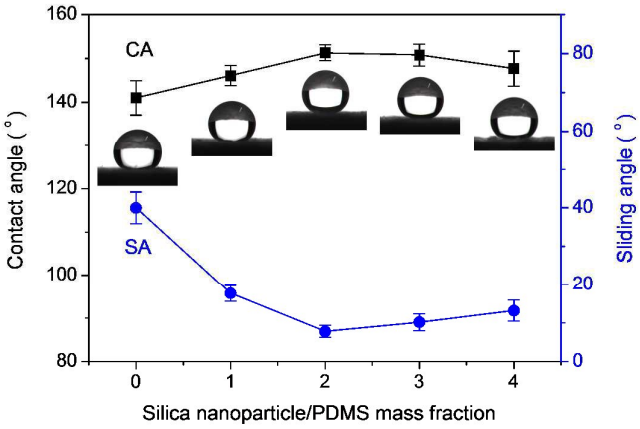

Fig. 7 Static contact angles (CAs) and sliding angles (SAs) of the coated wood as a function of silica nanoparticle/PDMS mass fraction. The typical images of water droplets on the surfaces are presented.

As shown in the optical photographs (Fig. 8a and b), spherical water droplets rested steadily on the superhydrophobic wood surface, which is in contrast to the instant penetration of water into the pristine wood. The prepared wood surface was not only superhydrophobic but also showed self-cleaning properties, which was demonstrated by dropping water to the carbon-powder contaminated wood surface (Fig. 8c-f). When dropped on the slightly tilted surface, the water droplets readily rolled off the superhydrophobic wood surface, carrying away the surface contaminants, whereas water droplets merged with the carbon powder and stuck on the pristine wood surface (see Video S1 and S2 in ESI†). However, it can be observed from Video S1 that some water droplets adhered to the superhydrophobic wood surface, which is mainly attributed to the structural heterogeneity of wood surfaces consisting of bright region of earlywood alternating with darker regions of latewood (see wood samples in Fig. 8a and b). The water droplets generally slid smoothly on the earlywood region while readily adhered to the narrow latewood region. This highlights the fact that it is more challenging to achieve superhydrophobicity on the heterogeneous wood surface as compared with the homogeneous substrates such as glass.

The wettability of a surface is governed by the surface composition as well as the microstructure. When the chemical composition is kept the same, the surface structure is the key factor affecting the surface wettability.[27] In the present study, the main function of silica particles in the hybrid coating system is to generate nanoscale roughness. Hence, the silica particle to PDMS mass ratio

is very critical to control the microstructure and roughness of the hybrid coatings, resulting in tunable water-repellent properties of the coated wood. The influence of roughness on the wettability of a surface has been primarily discussed in terms of the Wenzel and Cassie-Baxter models.[28,29] When the silica particle loading was low, the resulting hybrid coatings were not notably roughened, which appeared to impose little impact on the inherent microstructure of the wood surfaces. In this case, water droplets can fill and wet the open lumen space of the longitudinally arranged cells of the wood substrate, resulting in a large contact angle hysteresis, which could be described by the Wenzel model. However, in view of the relatively high CA values, it is reasonable to assume that water droplets may also be in the Cassie state, in which the solid-liquid contact area fraction is high and thus water droplet pinning can occur as indicated by the relatively large SAs.

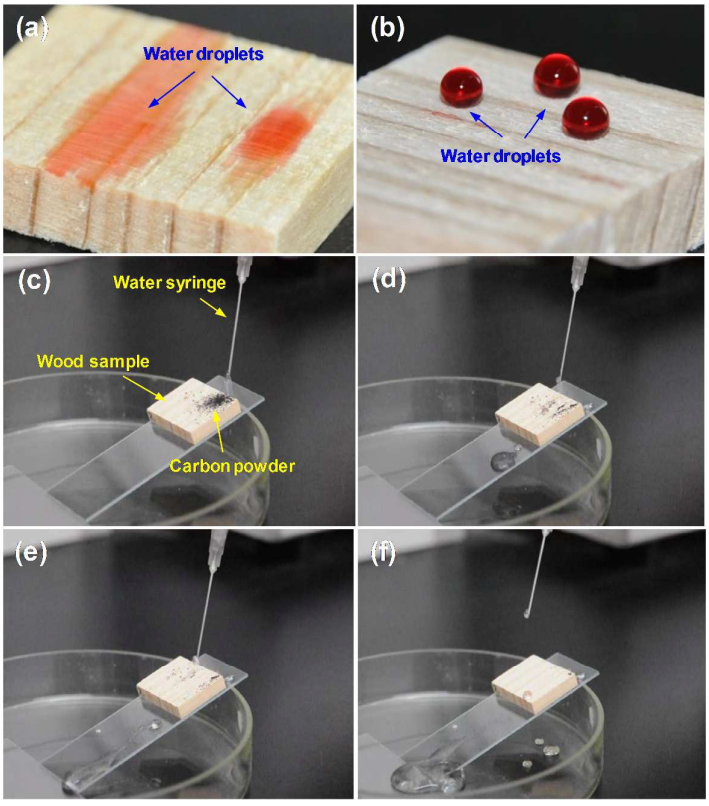

Fig. 8 Optical photographs of water droplets (mixed with a red dye) on the (a) pristine and (b) superhydrophobic wood surfaces; (c-f) snapshots of the self-cleaning process on the superhydrophobic wood surfaces.

By contrast, when the silica particle loading was raised to a certain level (*e.g.* silica/PDMS mass ratio is 2:1), the resulting hybrid coating appeared to develop a hierarchical microstructure with interconnected microdomains and nanopores, producing highly roughened wood lumen surfaces. Such a hierarchical structure with nanoscale roughness superimposed on the microscale roughness is known to be an essential feature in generating superhydrophobic properties and more important for achieving low water sliding angles.[30-33] Accordingly, water droplets could not wet the surface but are suspended over the hierarchical structure with large fraction of air being entrapped inside, which is a typical wetting behavior described by the Cassie model. Consequently, a higher CA (greater than 150°) was observed, and the adhesion force between the water droplets and the wood substrate was very small. In short, the surface roughness, which is tuned by changing the silica/PDMS ratio, plays a vital role in governing the surface wettability of the coated wood. The surface roughness has to exceed a critical level to transform into the "desired" Cassie state with a small contact angle hysteresis.

Mechanical durability of the superhydrophobic coatings

The major issue for the practical application of superhydrophobic wood is that the elaborately fabricated microstructures of the rough surfaces could be easily damaged by mechanical abrasion. Scratch tests were carried out to examine the abrasion resistance of the superhydrophobic coatings (SiO_2/PDMS mass ratio is 2:1) on wood surfaces. Fig. 9a shows the change in CAs and SAs as a function of abrasion cycles for the structured wood surface. It can be seen that the CAs of the coated wood remained almost constant around 150° after being scratched repeatedly, and spherical water droplets can still form on the surface. However, the mechanical abrasion caused an obvious increase in the SAs, and water droplets were not easy to roll, reflecting an increased contact angle hysteresis. SEM images show that the microscale structures on the wood surface were severely damaged by the mechanical abrasion with such a high loading pressure (12.5 kPa), whereas the nanoscale features of the PDMS/silica hybrid coating in the cell lumens was well retained in general (Fig. 9b). As schematically illustrated in Fig. 9c, once the inherent microscale bumps (protruded cell walls) of the wood surface has been partly worn out, the underlying hydrophilic bulk wood would be exposed as a result, introducing water pinning sites that consequently make the surface more sticky towards water. Nevertheless, despite an increase in the contact angle

hysteresis induced by the mechanical abrasion, the wood surface remained non-wettable with the nanoscale features being kept intact in general. It should be noted that the applied loading pressure (12.5 kPa) in this study is too harsh for the as-prepared superhydrophobic wood surface since the inherent microscale features of the surface were severely damaged.

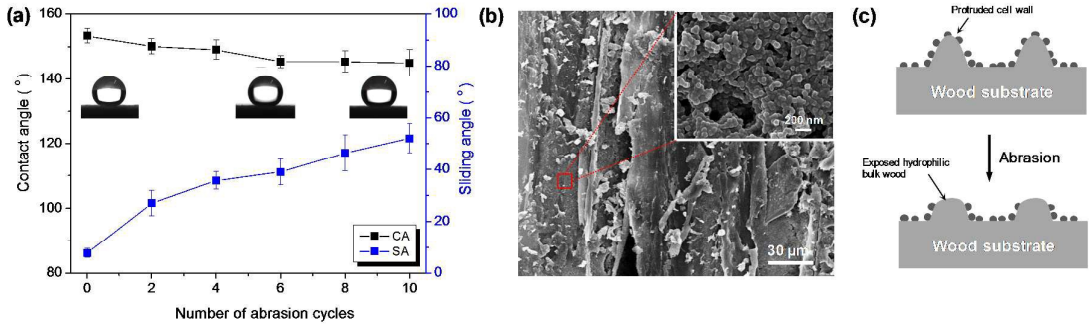

Fig. 9 (a) CAs and SAs as a function of number of abrasion cycles for the superhydrophobic wood surfaces; (b) SEM images of the wood surface after 10 abrasion cycles; (c) Sketch illustrating abrasion-induced damage to the microscale features (protruded cell walls) on the wood surface, exposing the hydrophilic bulk wood.

We also qualitatively assessed the mechanical stability of the superhydrophobic wood surfaces against finger touching. As shown in Fig. 10, the wood surface remained superhydrophobic upon being touched by a finger. Water droplets exhibited a spherical shape on the touched surface with a CA of ~150° and can easily roll off at a small tilting angle. This indicates that the surface textures were robust enough to withstand the force exerted by finger touching and also exhibited resistance against grease contamination caused by finger contact, making the surface a finger touchable superhydrophobic surface. In the hybrid coating system, PDMS was expected to function as a binding agent to aggregate the silica particles and anchor the particles tightly on the wood substrate, thus endowing the coatings with good mechanical stability.

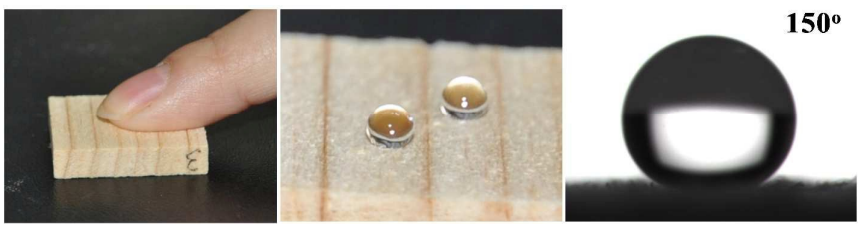

Fig. 10 The wood surface remained superhydrophobic upon being touched by a finger, and water droplets exhibited a spherical shape on the touched surface with a CA of 150°.

The durability of the superhydrophobic coatings was further examined by ultrasonic washing in water with a high ultrasonic frequency of 80 kHz. Fig. 11 shows the change in CAs and SAs as a function of ultrasonic washing time for the coated wood. It can be seen that the CAs of the coated remained almost constant around 150°, and SAs exhibited only a slight increase up to 12° after ultrasonic washing for a duration of 10 h. This indicates that the PDMS-anchored nanoparticles and the well-developed microstructure were resistant against the cavitation damage induced by the high frequency (80 kHz) ultrasound, and the hybrid coatings were therefore durable enough to withstand the ultrasonic impact without impairing its water-repellency.

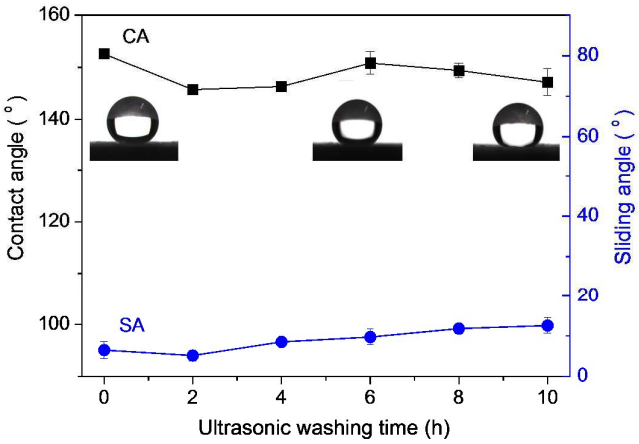

Fig. 11 CAs and SAs as a function of time of ultrasonic washing in water for the superhydrophobic wood surfaces.

Conclusions

In summary, a simple and inexpensive dip-coating method has been successfully applied to fabricate durable superhydrophobic organic-inorganic hybrid coatings on the intrinsically heterogeneous wood surfaces by using PDMS-silica nanocomposites. The surface morphology and microstructure of the hybrid coatings can be readily controlled by adjusting the silica particle loadings in the PDMS matrix, and the surface roughness and wettability of the coated wood was accordingly tuned. When silica/PDMS mass ratio was raised to 2:1, hierarchical microstructures with interconnected microdomains and nanopores were formed in the coating, allowing the generation of superhydrophobic wood surfaces. The fabricated PDMS/silica hybrid coating also showed desirable mechanical stability and durability against mechanical abrasion and

high-frequency ultrasonic washing in water, highlighting their potential in various practical applications.

Electronic Supplementary Information (ESI)

Video S1 showing water droplets rolling off the superhydrophobic wood surface, carrying away the surface contaminants, in contrast to Video S2 showing water droplets merged with the contaminants and stuck on the pristine wood surface.

Acknowledgements

The authors acknowledge the financial support from the Grant for National Non-profit Research Institutions of Chinese Academy of Forestry (CAFINT2011C05) and the National Natural Science Foundation of China (31170527).

References

1 C. A. S. Hill and D. Jones, *Holzforschung*, 1999, **53**, 267-271.

2 H. T. Chang and S. T. Chang, *Bioresource Technol.*, 2002, **85**, 201-204.

3 S. Donath, H. Militz and C. Mai, *Wood Sci. Technol*., 2004, **38**, 555-566.

4 S. Donath, H. Militz and C. Mai, *Holzforschung*, 2006, **60**, 40-46.

5 E. Cabane, T. Keplinger, V. Merk, P. Hass and I. Burgert, *ChemSusChem*, 2014, **7**, 1020-1023.

6 T. Keplinger, E. Cabane, M. Chanana, P. Hass, V. Merk, N. Gierlinger and I. Burgert, *Acta Biomater.*, 2015, **11**, 256-263.

7 M. A. Ermeydan, E. Cabane, A. Masic, J. Koetz and I. Burgert, *ACS Appl. Mater. Interfaces*, 2012, **4**, 5782-5789.

8 C. Neinhuis and W. Barthlott, *Ann. Bot*., 1997, **79**, 667-677.

9 L. Feng, Y. Zhang, J. Xi, Y. Zhu, N. Wang, F. Xia and L. Jiang, *Langmuir*, 2008, **24**, 4114-4119.

10 X. Gao and L. Jiang, *Nature*, 2004, **432**, 36.

11 R. Fürstner and W. Barthlott, *Langmuir*, 2005, **21**, 956-961.

12 L. Cao, A. K. Jones, V. K. Sikka, J. Wu and D. Gao, *Langmuir*, 2009, **25**, 12444-12448.

13 B. Bhushan, Y. C. Jung and K. Koch, *Phil. Tran. R. Soc. A*, 2009, **367**, 1631-1672.

14 B. Bhushan and Y. C. Jung, *Prog. Mater. Sci.*, 2011, **56**, 1-108.

15 Y. L. Zhang, H. Xia, E. Kim and H. B. Sun, *Soft Matter*, 2012, **8**, 11217-11231.

16 L. Feng, S. L, Y. Li, H. Li, L. Zhang, J. Zhai, Y. Song, B. Liu, L. Jiang and D. Zhu, *Adv. Mater.*, 2002, **14**, 1857-1860.

17 S. Wang, C. Liu, G. Liu, M. Zhang, J. Li and C. Wang, *Appl. Surf. Sci.*, 2011, **258**, 806-810.

18 X. Wang, Y. Chai and J. Liu, *Holzforschung*, 2013, **67**, 667-672.

19 Q. Sun, Y. Lu and Y. Liu, *J. Mater. Sci.,* 2011, **46**, 7706-7712.

20 Y. Fu, H. Yu, Q. Sun, G. Li and Y. Liu, *Holzforschung*, 2012, **66**, 739-744.

21 C. Wang, C. Piao and C. Lucas, *J. Appl. Polym. Sci.*, 2011, **119**, 1667-1672.

22 S. Wang, J. Shi C .Liu, C. Xie and C. Wang, *Appl. Surf. Sci.*, 2011, **257**, 9362-9365.

23 B. Poaty, B. Riedl, P. Blanchet, V. Blanchard and L. Stafford, *Wood Sci. Technol.*, 2013, **47**, 411-422.

24 X. Zhu, Z. Zhang, X. Men, J. Yang, K. Wang, X. Xu, X. Zhou and Q. Xue, *J. Mater. Chem.*, 2011, **21**, 15793-15797.

25 Q. Ke, W. Fu, S. Wang, T. Tang and J. Zhang, *ACS Appl. Mater. Interfaces*, 2010, **4**, 2393-2398.

26 T. Nishino, M. Meguro, K. Nakamae, M. Matsushita and Y. Ueda, *Langmuir*, 1999, **15**, 4321-4323.

27 Q. F. Xu, J. N. Wang and K. D. Sanderson, *ACS Nano*, 2010, **4**, 2201-2209.

28 R. N. Wenzel, *Ind. Eng. Chem.*, 1936**, 28**, 988-994.

29 A. B. D. Cassie and S. Baxter, *Trans. Faraday Soc.*, 1944, **40**, 546-551.

30 N. A. Patankar, *Langmuir*, 2004, **20**, 7097-7102.

31 W. Ming, D. Wu, R. Benthem and G. With, *Nano Lett.*, 2015, **5**, 2298-2301.

32 D. Quéré, *Annu. Rev. Mater. Res.*, 2008, **38**, 71-99.

33 X. Deng, L. Mammen, H. J. Butt and D. Vollmer, *Science*, 2012, **335**, 67-70.